



Preparation of H₃PO₄ activated carbon from *Ziziphus lotus* (*Z. mauritiana*) leaves: Optimization using RSM and cationic dye adsorption

Asmaa Msaad^{a,*}, Mounir Belbahloul^a, Samir El Hajjaji^b, Abdeljalil Zouhri^a

^aUniversity Hassan I, Chemistry and Environment Laboratory, Faculty of Science and Technology, BP 577, Settat 26000, Morocco, email: *asmaa.msd@gmail.com (A. Msaad), belbahloulmounir@yahoo.fr (M. Belbahloul), abdzouhri@yahoo.fr (A. Zouhri)

^bAl Akhawayn University in Ifrane, School of Science & Engineering, Hassan II avenue, Ifrane 53000, Morocco, Tel. +212535862330, email: s.elhajjaji@au.ma (S. El Hajjaji)

Received 24 August 2018; Accepted 22 January 2019

ABSTRACT

An experimental study on the adsorption of Methylene Blue (MB) onto *Ziziphus lotus* (ZL) leaves-based raw and activated carbon (AC) is presented herein. The optimization of AC production conditions and adsorption process parameters were performed by Box-Behnken design. Parameters tested for AC production optimization are chemical impregnation ratio (1–3 w/w), activation temperature (200–800°C), and holding time (30–120 min). While, the adsorption optimization parameters are pH (2–12), adsorbent dosage (10–100 mg), and contact time (10–80 min). The regression analysis showed a good fit of the experimental data to the second-order polynomial model. Optimal conditions of production of ZL AC were found to be a temperature of 413°C, an impregnation ratio of 2.76 w/w and a contact time of 71.85 min. Those of MB adsorption on raw material and AC successively are: an adsorbent dosage of 769/392 mg/L, a pH of 10.4/11.9 and a contact time of 38.60/32.75 min.

Keywords: *Ziziphus lotus*; Activated carbon; Methylene Blue; Adsorption; Box-Behnken

1. Introduction

Industrial wastewater is the result of a number of processes. In Morocco alone, a total volume of 931 Mm³ is rejected by the chemical and para-chemical industries every year [1]. One pollutant of interest that is commonly found in these wastewaters is dye. Among the 100,000 dyes commercially available, 70 wt% are synthetic azoic dyes [2], 10% of which are released directly into the environment. Methylene blue (MB), a cationic dye which is the subject of this study, is most commonly used for coloring and in the textile industry. Owing to its high water solubility, wastewater containing MB is hazardous to the environment and human health. It causes a noticeable coloration and is classified as a toxic colorant at concentrations as low as

1 mg/L [3]; furthermore, it reduces light penetration and precludes the photosynthesis of aqueous flora and oxygenation of water reservoirs. Harmful impacts on health include eye irritation, gastrointestinal irritation and nausea upon ingestion, vomiting and diarrhea [4]. It is therefore clear that treatment of this hazardous dye is a real environmental and health challenge.

To face this challenging situation, one must seek an appropriate method that takes into account local constraints and regulations. Dye removal techniques reported in the literature include coagulation, chemical oxidation, electrochemical methods [5], and finally adsorption which is attractive because of its lower cost, high efficiency and easy operation [5,6]. Nowadays, a wide range of applications has been found for activated carbons in adsorption processes in order to remove color, odor and taste from water and wastewater, to recover natural gas, to purify air in the chemical and petrochemical industries, and to act as

*Corresponding author.

catalysts and catalyst supports [7,8]. Commercial activated carbons currently available in the market have proven to be effective in the removal of dyes from wastewater, but their high cost has brought about the search for more economically competitive alternatives [9]. Low-cost adsorbents, characterized by a large surface area and a good conductivity, have been highlighted in recent studies [10]; they can be produced from a variety of sources including *Manihot esculenta* Crantz waste [11], rubber seed shell [12], walnut shell [13], chitosan derivatives [14], rice husk [15], herbs from the Apiaceae family [16], polyaniline coated calcined layered double hydroxides [17], modified bentonite [18], crushed bricks [19], alginate crosslinked *Prunus avium* leaves [20] and soybean straw [21].

Ziziphus lotus (ZL) is a deciduous, thorny shrub of the Rhamnaceae family, occurring throughout most of the Mediterranean region and eastward to the Red Sea coast [22,23]. Interestingly, valorization and usage of ZL leaves as adsorbents remains unreported to date. In fact, the only application of ZL reported in the literature in the field of wastewater treatment concerns the use of jujube shells of ZL as a sorbent in the removal of Congo red from aqueous solutions [24]. In that context, the study reported herein investigates the optimization of the preparation of a low-cost and eco-friendly ZL-based activated carbon and its subsequent application in the treatment of MB wastewater.

Activation of the ZL raw material was done chemically using H_3PO_4 . Indeed, to reach a high performance, biomass-based adsorbents should be activated either by physical or chemical means. On the one hand, physical activation generates large amounts of volatile matter and requires high energy consumption. On the other hand, chemical activation which is a process involving dehydrogenation reactions reduces significantly the amount of volatile substances generated [25]. The activating agent helps to develop the activated carbon porosity by dehydration and degradation. Certain dehydrating agents affect the temperature of pyrolysis and inhibit the formation of tar, thus increasing the carbon yield [26]. Examples of chemical activating agents include phosphoric acid (H_3PO_4), zinc chloride ($ZnCl_2$) and potassium hydroxide (KOH) among others. H_3PO_4 and $ZnCl_2$ have been used extensively for biomass precursors while KOH is rather preferred for coal-based precursors. H_3PO_4 acts as a dehydrating catalyst that promotes the decomposition of the cellulosic precursor at relatively low activation temperatures, which restricts tar formation, cross-linking, and inhibits the shrinkage of the precursor particle [27]. In addition, this acid is environmentally friendly, easy to recover, and amenable to recycling [28–30]. Finally, another important asset of H_3PO_4 activation is the development of mesoporous carbons, which is suitable for the adsorption of large molecules [31].

In this work, conditions of MB adsorption, on both raw and chemically activated carbon adsorbents made from ZL, were determined using the response surface methodology (RSM) by altering three parameters. RSM uses a Box-Behnken experimental design, a standard statistical tool mostly used for process optimization with a minimum number of experiments; it evaluates simple and combined effects of different variables on the response of several dye removal processes [32,33].

Characterization of the adsorbents by Fourier Transform Infrared Spectroscopy (FTIR), Scanning Electron Microscopy (SEM), BET surface area and X-Ray Diffraction (XRD) was performed to get insight on their efficacy for MB removal.

2. Materials and methods

2.1. Raw material

ZL leaves were obtained from the Settat-Casablanca region located in Morocco. These leaves were washed several times with distilled water to remove residues, and dried at 75°C in an oven for 24 h. The bio-material was then ground and stored in a closed glass container for later use as adsorbent, as is [34] or in the activated form using phosphoric acid.

2.2. Preparation of activated carbon

ZL activated carbon was prepared using the raw ground and sieved material. To determine the optimal production conditions of the sorbent, three factors influencing the preparation were selected: impregnation ratio material: H_3PO_4 (1–3 w/w), temperature interval (200–800°C), and contact time (30–120 min). The percentage of dye removal was the parameter chosen as a “response”, in order to optimize the activated carbon preparation conditions.

2.3. Reagents

The dye used in this study is Methylene Blue (MB) $C_{16}H_{18}ClN_3S$, an azoic dye characterized by a maximum absorbance wavelength of 663 nm. Reagents employed in the various steps of this process are: H_3PO_4 , 0.1 N HCl and 0.1 N NaOH.

2.4. Adsorption experiments

Adsorption experiments were performed in a batch-adsorption system. MB removal experiments were conducted by varying the process parameters: pH, adsorbent dosage and contact time. pH of the solution was adjusted with 0.1 N aqueous solutions of NaOH and HCl. Different adsorbent doses of *Ziziphus Lotus* raw material or activated carbon were added to 100 mL of MB solution (100 mg/L), then, the samples were withdrawn at appropriate time intervals, and centrifuged at 7500 rpm for 2 min. The residual MB concentration was determined using a UV/VIS spectrophotometer set at 663 nm. The percentage of MB removal was calculated according to Eq. (1):

$$R(\%) = \frac{C_0 - C_t}{C_0} \times 100 \quad (1)$$

where C_0 is the initial concentration of MB solution (mg/L) and C_t is the MB concentration at time t (mg/L).

2.5. Response surface modeling

Response surface modeling (RSM) is an empirical statistical technique that uses quantitative data obtained

from appropriately designed experiments to determine a regression model and operating conditions [35,36]. The main objective of RSM is to determine the optimum set of operational variables of the process [37], and its approach has been widely applied in chemical engineering and adsorption process optimization [38]. In light of these assets, RSM was utilized in this study as an optimization tool for the production of ZL activated carbon and its application in the removal of MB from aqueous solution. Experiments were carried out according to a Box–Behnken design to obtain the experimental data which would fit an empirical full second-order polynomial model representing the response surface over a relatively broad range of parameters. The Box–Behnken design of the activated carbon preparation conditions and MB decolorization efficiency are shown in Table 1 and Table 6 respectively. The data was evaluated by analysis of variance (ANOVA) using NemrodW® version 2007.3. A total of 17 experiments were necessary to estimate the model with: three factorial points, five central points and a 99% confidence interval.

2.6. Characterization of adsorbents

The morphology and microstructure of the ZL raw material and activated carbon were studied by scanning electron microscopy (FEI FEG 450 microscope) and the surface properties and surface area were determined by a Micromeritics analyzer model 3Flex 3500. Surface functional groups of adsorbents were characterized using Fourier Transform Infrared Spectroscopy using a SHIMADZU FTIR-8400S spectrometer. Finally, X-ray diffraction measurements were done using a D2 PHASER-BRUKER diffractometer.

Table 1
Box–Behnken design matrix with experimental responses

Experiment	Impregnation ratio (X_1)	Activation temperature (X_2)	Holding time (X_3)	MB Removal (%)
1	-1	-1	0	45.00
2	1	-1	0	96.11
3	-1	1	0	97.98
4	1	1	0	99.25
5	-1	0	-1	98.26
6	1	0	-1	96.98
7	-1	0	1	0.51
8	1	0	1	22.28
9	0	-1	-1	97.63
10	0	1	-1	96.81
11	0	-1	1	0.26
12	0	1	1	53.37
13	0	0	0	98.23
14	0	0	0	98.24
15	0	0	0	98.22
16	0	0	0	98.23
17	0	0	0	98.24

3. Results and discussion

3.1. Optimization of activated carbon preparation conditions

3.1.1. Box–Behnken design and variables levels

In the present work, 17 experiments using the Box–Behnken design with three factors and five central points were studied. Variables of the activated carbon preparation were: chemical impregnation ratio (X_1), activation temperature (X_2), and holding time (X_3). Factors affecting the production of activated carbon from ZL leaves were studied with standard RSM in order to identify and optimize the effective process parameters [39]. The upper limit, central point and lower limit of the variables coded '1', '0', and '-1' are [1, 2, 3 w/w], [200, 500, 800°C] and [30, 75, 120 min] respectively. Conditions and results of the experiment are listed in Table 1. The linear equation, which is expressed by Eq. (2), assumes a relationship between the three factors and the experimental response (percentage of MB removal).

$$Y = b_0 + \sum_{i=1}^n biXi + \sum_{i=1}^n biiXi^2 + \sum_{ij} bijXiXj \quad (2)$$

where Y is the experimental response; X_i, X_j are coded independent variables; b_0 is the constant coefficient; b_i is the linear term coefficient; b_{ii} is the squared effect; and b_{ij} is the interaction coefficient.

3.1.2. Statistical validation of the Box–Behnken model

The adequacy of the selected model and statistical significance of the regression coefficients were tested using ANOVA and the F-test [40]. The analysis of variance for the response is predicted in Table 2. To evaluate the model, the coefficient of Response Surface Modeling of ZL activated carbon preparation, the ratio of the standard error of estimate of the mean value and F-value tests were also performed. As a general rule, if p-value is less than 0.05, the model parameter is significant. On the basis of ANOVA, it can be concluded that the selected model adequately represents the data for activated carbon preparation. Comparison of the experimental values with the predicted ones shows a perfect match, with a value of R^2 of 0.99, meaning that 99% of the results are explained by the model. The larger value of F and the smaller p-value indicate that most of the variation in the response can be explained by the regression equation. From the ANOVA results, it can be concluded that the model predictions using the Box–Behnken mathematic model is suitable and can be utilized to identify the optimum process conditions.

This model shows that the impregnation ratio, time and temperature have a negative effect on the percentage of MB removal (Table 3). An increasing impregnation ratio decreases the MB removal efficiency while increasing carbon burn-off. When a higher H_3PO_4 impregnation ratio was used, weight losses were due to the increase of volatile products released as a result of intensification in the dehydration and elimination reactions [36]. As for the detrimental effect of temperature, it is explained by the fact that, at higher temperature more volatiles are released, and impurities in the sample generated by thermolysis result in a lower MB removal capacity. This phenomenon has been described

Table 2
ANOVA regression for *Ziziphus lotus* activated carbon

Source	DF	Adj SS ^(a)	Adj MS ^(b)	F-value	p-value
Model	9	21274.9	2363.9	65.12	0
Linear	3	14399.3	4799.8	132.23	0
A	1	663.8	663.8	18.29	0.004
B	1	1469.1	1469.1	40.47	0
C	1	12266.5	12266.5	337.93	0
Square	3	5394.7	1798.2	49.54	0
A×A	1	471.1	471.1	12.98	0.009
B×B	1	39.6	39.6	1.09	0.331
C×C	1	4625.6	4625.6	127.43	0
2-way interaction	3	1480.9	493.6	13.60	0.003
A×B	1	621	621	17.11	0.004
A×C	1	132.8	132.8	3.66	0.097
B×C	1	727.1	727.1	20.03	0.003
Error	7	254.1	36.3		
Lack-of-fit	3	0	84.7	1693942.17	0
Pure error	4	21529	0		
Total	16				

(a) Adjusted sums of squares

(b) Adjusted mean squares

Table 3
Estimation of coefficients

Name	Coefficient	Standard deviation	Significance (%)
b0	98.234	0.00244948	< 0.01
b1	8.484	0.00193649	< 0.01
b2	13.426	0.00193649	< 0.01
b3	-39.408	0.0019364	< 0.01
b1-1	-10.455	0.00266926	< 0.01
b2-2	-3.445	0.00266926	< 0.01
b3-3	-33.272	0.00266926	< 0.01
b1-2	-11.210	0.00273861	< 0.01
b1-3	5.763	0.00273861	< 0.01
b2-3	12.982	0.00273861	< 0.01

in the literature; in studies employing $ZnCl_2$ chemical activation for example [41,42]. A statistical analysis of the Box-Behnken model can be used for modeling the experimental system. The model can be described by Eq. (3).

$$R(\%) = 98.23 + 8.48X_1 + 13.42X_2 - 39.40X_3 - 11.21X_1X_2 + 5.76X_1X_3 + 12.98X_2X_3 - 10.455X_1^2 - 3.44X_2^2 - 33.272X_3^2 \quad (3)$$

3.1.3. Three-dimensional response surface plots

The three-dimensional surface and contour map of interactions between pairs of factors varying within their experimental ranges, while maintaining all others param-

eters at fixed levels (center), provides information on the relationship between factors, and their interaction effects [43]. Fig. 1 shows the response plot indicating the effects of ratio (X_1), temperature (X_2) and time (X_3) on the percentage of MB removal.

Fig. 1a suggests that the interaction between effect of time and ratio influences the percentage of MB removal negatively. The 3D plot showing the effect of temperature (X_2) and time (X_3) on MB removal is shown in Fig. 1b; according to this plot, increasing the temperature at a fixed impregnation ratio value will decrease the MB removal percentage due to excessive carbon burn-off, thus resulting in the widening of pores and even the loss of walls between these pores [44]. Finally, Fig. 1c shows the 3D plot of ratio and temperature; it indicates that increasing temperature and time increase the percentage of MB removal.

3.1.4. Preparation optimization and experimental model validation of ZL activated carbon

The RSM could therefore be successfully applied to find the optimum process parameters at which the activated carbon produced has its highest MB removal capacity. Optimized conditions were found to be: a ratio of 2.76 w/w, a temperature of 413°C, and a time of 71.85 min to reach a MB removal of 99.59%. To finalize the modeling process, model validation was carried out. To this end, five experiments were run using the optimal conditions previously determined. A mean value of 99.59 ± 0.1% was found, which is in agreement with the predicted value. The results confirm that the model is very significant to optimize the activated carbon preparation conditions.

3.2. Characterization of *Ziziphus lotus* raw material and activated carbon

3.2.1. FTIR spectroscopy analysis

FTIR spectra were obtained to evaluate qualitatively the chemical structures of the ZL raw material and activated carbon (Fig. 2).

The FTIR spectrum of the raw material (Fig. 2a) shows various surface functional groups. It reveals a broad band around 3300 cm^{-1} that can be attributed to the hydroxyl groups -OH of lignin [45] and the hydrogen-bonded OH vibration of the cellulosic structure [46]. Bands at around 2900 cm^{-1} correspond to C-H stretching vibration, while those at around 1618 cm^{-1} could be attributed to the stretching of aromatic rings (C=C) [47]. The stretching vibration of the molecular plane of C-C bands, characteristic of aromatic rings arises in the region of 1465 cm^{-1} [48]. The band between 1300 cm^{-1} and 1100 cm^{-1} is partly associated with C-O stretching and O-H bending modes in the functional group [49,50]; the band at around 1028 cm^{-1} can be attributed to the C-OH stretching of phenolic groups [51]. The band caused by O-H of cellulose is located between 400–700 cm^{-1} [52]. The presence of carbonyl group, hydroxyl groups, and aromatic compound is a confirmation of the lignocellulosic structure. The FTIR spectrum of the activated carbon

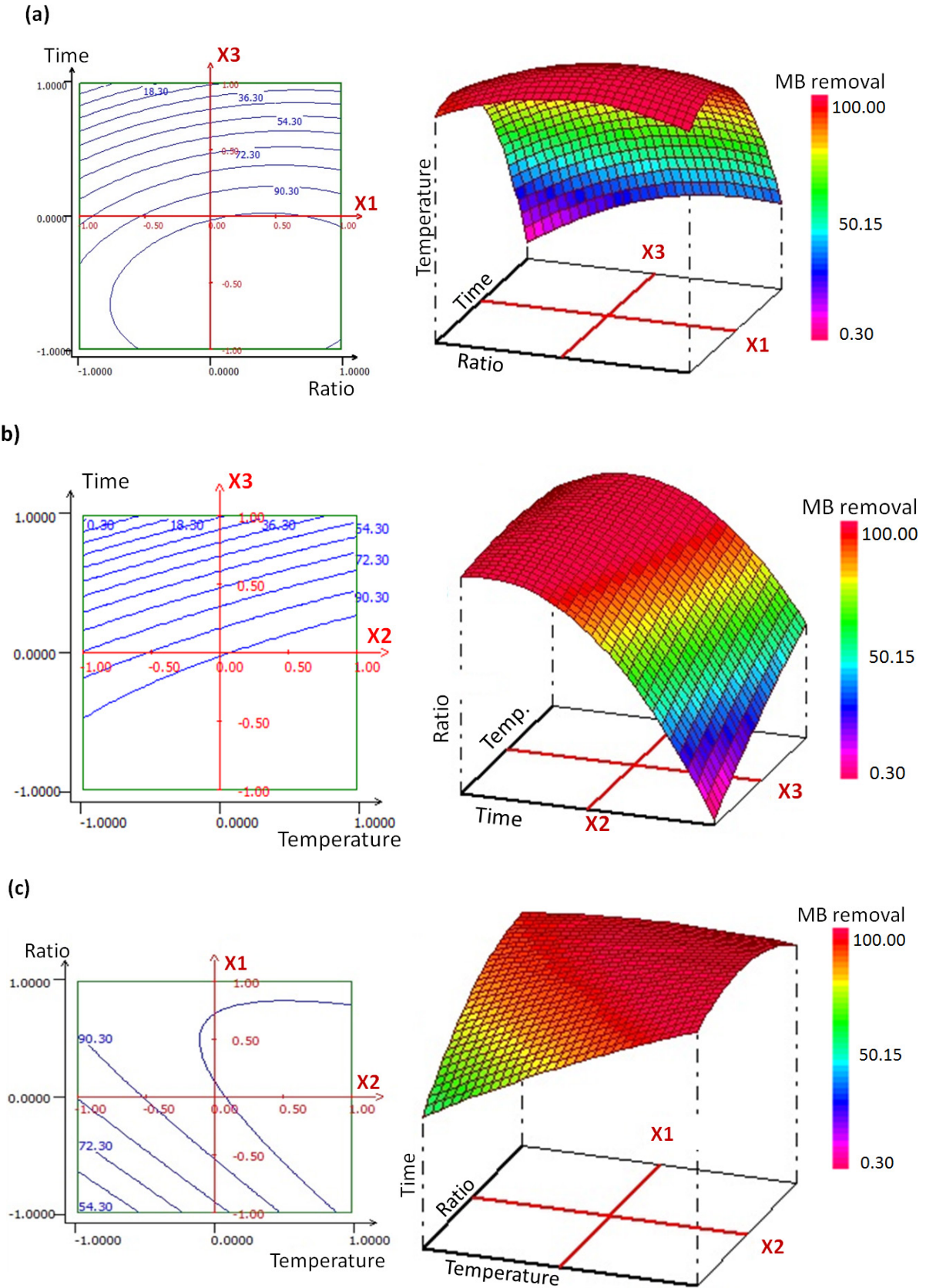


Fig. 1. 3D response surface plots showing the interactive effect of: (a) time and ratio, with temperature at the level of 0; (b) temperature and time, with ratio at the level of 0; (c) ratio and temperature, with time at the level of 0.

obtained is shown in Fig. 2b. Comparison of the spectra of the activated carbon and the raw material indicates that bands located at 1028, 2900, 1465 and 1300 cm^{-1} have disappeared, thus providing evidence that chemical bonds were broken during the activation and carbonization processes. In addition, evidence of a decrease in the functionality of the raw material is given by the decrease in the number of the other IR bands. The presence of lignin and cellulose structures suggest a lignocellulosic structure of raw and activated carbon from ZL; this structure is also observed in other carbon sources such as Brazilian coconut shell [53] and Tunisian olive-waste cakes [54]. It is known that active sites whereby attachment of ions occurs are polyphenolic compounds like the lignin groups present in lignocellulose [55]. Use of these materials in their natural state, without any treatment, has been reported to cause problems of lower durability, leaching of soluble organic components in strong acidic and basic media, and lower adsorption capacity [56].

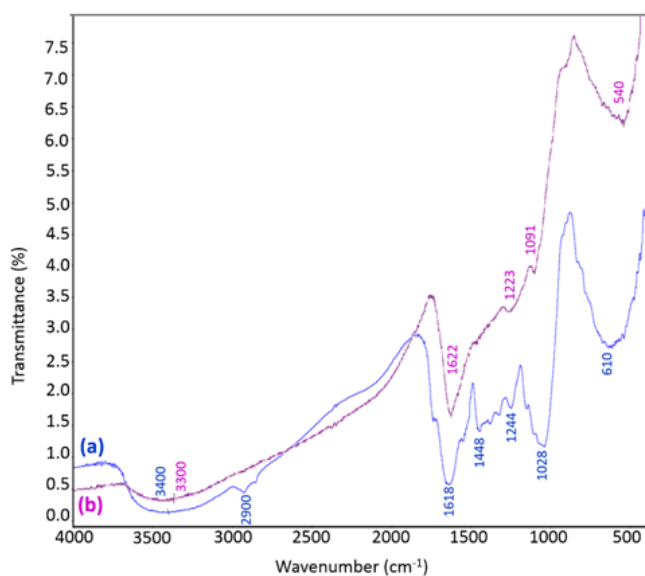


Fig. 2. FTIR spectra of ZL leaves: (a) raw material, (b) activated carbon.

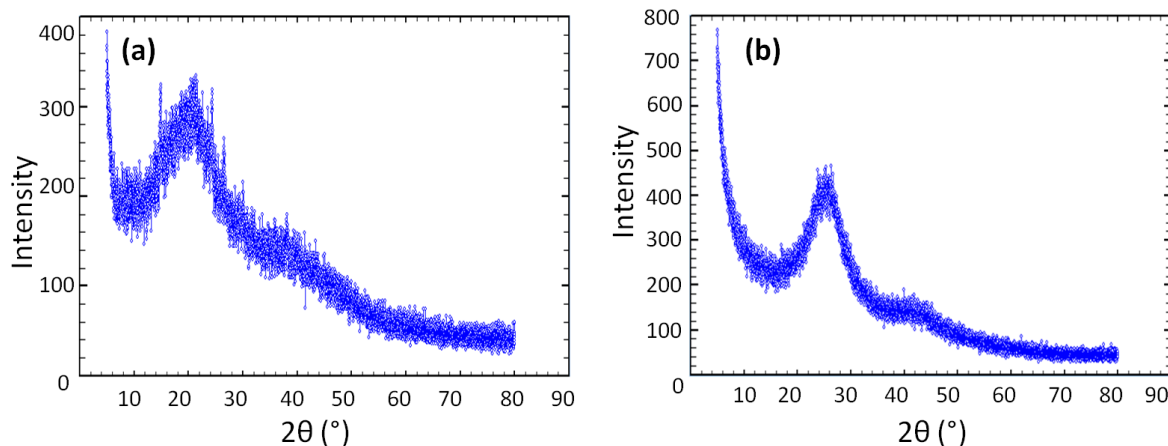


Fig. 3. XRD spectra of ZL: (a) raw adsorbent and (b) activated carbon.

3.2.2. XRD analysis

XRD spectra of untreated ZL (Fig. 3a) and activated carbon (Fig. 3b) adsorbents were acquired; they display a broad diffraction background and the absence of a sharp peak reveals a predominantly amorphous structure [57]. Amorphous peaks with equivalent Bragg angles (2θ) of 20° and 25° for raw material and activated carbon respectively were recorded. The amorphous structure of activated carbon has been reported for several products such as oil palm, empty fruit bunch and coconut shell [58].

3.2.3. BET analysis

Adsorption-desorption studies of nitrogen on ZL adsorbents were conducted to characterize their pore structure. Nitrogen adsorption and desorption isotherm curves are shown in Fig. 4. Nitrogen adsorption isotherms show a typical International Union of Pure and Applied Chemistry (IUPAC) type I pattern for ZL activated carbon (Fig. 4b) and an IUPAC type III pattern for the raw material (Fig. 4a). Fig. 4b illustrates a monolayer adsorption and suggests that the ZL activated carbon material is a microporous solid having relatively small external surfaces and that the limiting uptake is governed by the accessible micropore volume rather than the internal surface area. The ZL raw material is characterized by a type III isotherm, with a hysteresis loop, showing the presence of micropores. The Brunauer–Emmett–Teller (BET) surface area was calculated by the multiple-point method and was found to be 0.678 and 553.39 m^2/g for the ZL raw material and activated carbon respectively.

It should be noted that the surface area of ZL activated carbon is higher than that of the raw material; this result is due to the H_3PO_4 activation process. Comparison between the surface areas of the prepared activated carbon and other types of activated carbons is given in Table 4. S_{BET} of the prepared material is higher than the value of 377 m^2/g reported by Wang et al. [59] using activated carbon from sewage sludge. It is however closer to commercial activated carbon which has reportedly a value of 564 m^2/g [60]. Comparatively, Anisuzzaman et al. [61] found 966.74 m^2/g using activated carbon from *Typha orientalis* leaves. Generally, adsorption capacities increase with the increase of this parameter, so we can predict the effectiveness of the activated carbon [62].

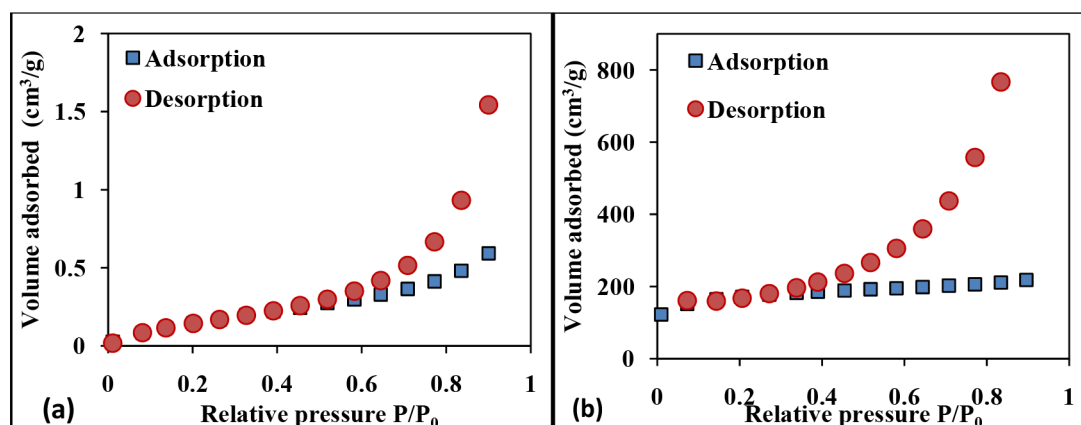


Fig. 4. Nitrogen adsorption-desorption isotherms of ZL: (a) raw material, (b) activated carbon.

Table 4
Comparison of the surface areas of activated carbons

Product	Preparation conditions and method	Surface area	Reference
Activated carbon from <i>Ziziphus lotus</i> leaves	H ₃ PO ₄ chemical activation. Impregnation ratio: 2.76 (w/w), temperature: 413°C, time: 71.85 min.	553.39 m ² /g	This work
Activated carbon from <i>Typha orientalis</i> leaves	Physical and H ₃ PO ₄ chemical activation. Semi-carbonization stage at 200°C for 15 min followed by activation at 500°C for 45 min.	966.74 m ² /g	[62]
Commercial activated carbon: high-purity powder (Sigma Aldrich)	–	564 m ² /g	[61]
Activated carbon from sewage sludge	H ₃ PO ₄ chemical activation. Impregnation ratio: 1.5 (w/w), drying at 105°C for 24 h, and heating in a microwave furnace at 800 W under a nitrogen flow of 10 mL/min for 10 min.	377 m ² /g	[60]

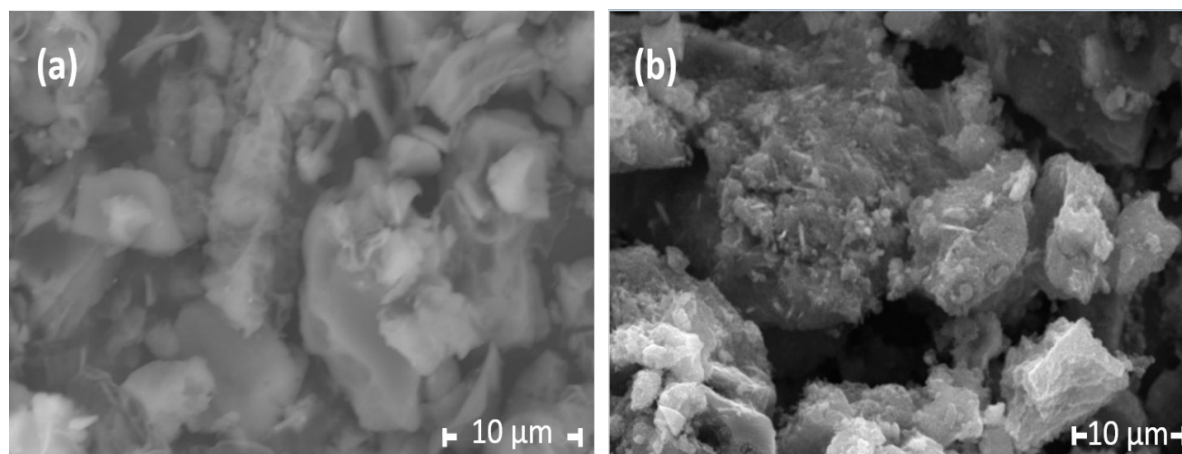


Fig. 5. SEM micrographs of ZL leaves: (a) raw material, (b) activated carbon.

3.2.4. SEM analysis

Fig. 5 presents SEM micrographs of ZL raw adsorbent and activated carbon.

Concerning activated carbon prepared from ZL leaves (Fig. 5b), the excellent capacity for removing pollutants from solution using the activated carbon is presumably due to the peculiar pore size distribution in this adsorbent developed during the chemical activation step [63].

3.3. Optimization of Methylene Blue adsorption parameters

pH of the solution, adsorbent dosage and contact time are three important factors affecting the adsorption process. Consequently, these parameters were selected as the independent variables to determine the best MB removal conditions using the ZL raw material and activated carbon as a low-cost adsorbent. An initial MB concentration of 100 mg/L was taken as a fixed input

Table 5
Variables and levels considered for percentage of removal of MB

Factor	Unit	ZL raw material		ZL activated carbon	
		High level (+1)	Low level (-1)	High level (+1)	Low level (-1)
pH	–	12	2	12	2
Adsorbent dosage	mg/100 mL	100	10	40	10
Contact time	min	80	10	60	10

Table 6
Box-Behnken design for the optimization of the MB removal process

Experiment	Impregnation ratio (X_1)	Activation temperature (X_2)	Holding time (X_3)	MB removal (%) with raw material	MB removal (%) with activated carbon
1	-1	-1	0	2.85	15.5
2	1	-1	0	36.80	35.2
3	-1	1	0	80.00	90.8
4	1	1	0	98.19	90.4
5	-1	0	-1	45.28	44.9
6	1	0	-1	84.40	53.4
7	-1	0	1	58.90	43.0
8	1	0	1	84.90	61.1
9	0	-1	-1	17.10	2.8
10	0	1	-1	90.29	87.0
11	0	-1	1	23.90	15.8
12	0	1	1	96.20	92.1
13	0	0	0	60.40	87.1
14	0	0	0	60.39	87.2
15	0	0	0	60.39	87.2
16	0	0	0	60.40	87.1
17	0	0	0	60.39	87.2

parameter (Table 5). Experimental results are shown in Table 6.

3.3.1. Statistical analysis

The analysis of variance for the response is given in Table 7. The good fit of the models for the raw and activated carbon was tested by the correlation coefficient (R^2).

The high values of R^2 of 0.998 and 0.991 for the activated carbon and the raw material respectively indicate that most of the data variation is explained by the regression model [64]. Also, we observed high values in the F-test and very low probability values ($p < 0.01$), which demonstrates that the model is highly significant [65].

3.3.2. Three-dimensional response surface plots

To understand the interaction effects of the parameters influencing the adsorption process, three-dimensional response surfaces were developed for the raw material (1) and ZL prepared activated carbon (2). Response surface plots are shown in Fig. 6.

Fig. 6a shows the combined effect of pH and adsorbent dosage on the adsorption of the dye at constant contact time for the raw and activated ZL leaves. The dye adsorption increases with both the solution pH and adsorbent dosage within their respective experimental range; the positive effect of adsorbent dosage can be explained by the increase of the number of binding sites for the dye molecules on the adsorbent surface [66]. The combination of the effects of pH and time (Fig. 6b) shows that the removal of MB increases with the increase of both pH and time; this phenomenon may be simply explained by the existence of a coulombic attraction between the positive charges of MB and the negative charges of the adsorbent as pH increases. The interactive effect of contact time and adsorbent dosage on adsorption at constant pH is shown in Fig. 6c; it is evident that adsorption increases with increasing contact time and adsorbent dosage.

3.3.3. Optimization and validation of MB adsorption conditions

Optimal conditions for the adsorption process using the ZL leaves raw material and activated carbon were deter-

Table 7
ANOVA analysis of ZL raw and activated carbon

	Source	DF	Adj SS ^(a)	Adj MS ^(b)	F-value	p-value
Raw material	Model	9	12441	1382.3	353.84	0
	Linear	3	11892.8	3964.3	1014.75	0
	A	1	1718.7	1718.7	439.95	0
	B	1	10084.1	10084.1	2581.28	0
	C	1	90	90	23.03	0.002
	Square	3	442.9	147.6	37.79	0
	A×A	1	32.6	32.6	8.34	0.023
	B×B	1	319.8	319.8	81.87	0
	C×C	1	113.6	113.6	29.08	0.001
	2-way interaction	3	105.3	35.1	8.99	0.008
	A×B	1	62.1	62.1	15.89	0.005
	A×C	1	43	43	11.02	0.013
	B×C	1	0.2	0.2	0.05	0.828
	Error	7	27.3	3.9		
	Lack-of-fit	3	27.3	9.1	303848.61	0
	Pure error	4	0	0		
	Total	16	12468.4			
Activated carbon	Model	9	15430.6	1714.5	86.91	0
	Linear	3	10919.9	3640	184.52	0
	A	1	263.4	263.4	13.35	0.008
	B	1	10585.1	10585.1	536.60	0
	C	1	71.4	71.4	3.62	0.099
	Square	3	4371.1	1457	73.86	0
	A×A	1	825.9	825.9	41.87	0
	B×B	1	970.2	970.2	49.19	0
	C×C	1	2142	2142	108.59	0
	2-way interaction	3	139.6	46.5	2.36	0.158
	A×B	1	101	101	5.12	0.058
	A×C	1	23	23	1.17	0.316
	B×C	1	15.6	15.6	0.79	0.403
	Error	7	138.1	19.7		
	Lack-of-fit	3	138.1	46	15341.39	0
	Pure error	4	0	0		
	Total	16	15568.7			

(a) Adjusted sums of squares (b) Adjusted mean squares

mined by using the quadratic model. pH, adsorbent dosage and contact time defining these conditions are shown in Table 8.

Table 8 summarizes values corresponding to optimal conditions. For their validation, five experiments were conducted using the optimized parameters obtained. A mean value of $99.56 \pm 0.10\%$ and $99.19 \pm 0.12\%$ were found experimentally, which is in accordance with the predicted value. So the model is very significant to optimize the MB adsorption conditions.

4. Conclusion

This study was carried out to prepare activated carbon from ZL leaves and identify the optimal conditions to remove MB from aqueous solutions using the ZL raw material and activated carbon using the RSM method:

The optimum conditions of preparation of ZL activated carbon were found to be a ratio of 2.76 w/w, a temperature of 413°C, and a time of 71.85 min.

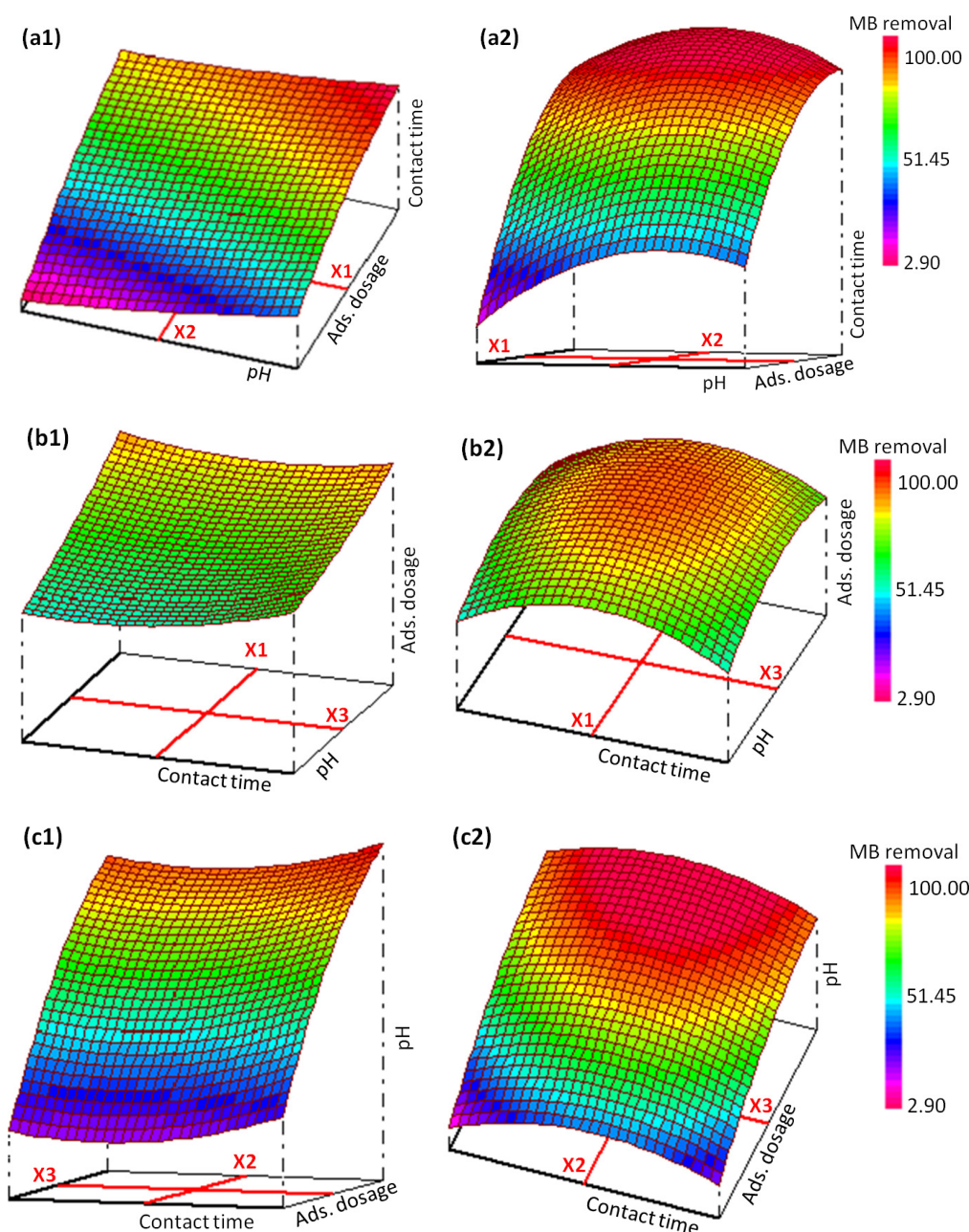


Fig. 6. Response surface plots showing effect of (a) pH and adsorbent dosage, (b) pH and contact time, (c) adsorbent dosage and contact time, on MB removal by untreated and activated ZL leaves. 1 = raw material, 2 = activated carbon.

Table 8
Optimal conditions for MB removal using the ZL leaves raw material and activated carbon. MB solution used: $V = 100$ mL, initial concentration = 100 mg/L.

	pH	Adsorbent dosage (mg/100 mL)	Contact time (min)	MB removal (%)
Untreated ZL adsorbent	10.4	76.9	38.6	99.19
Activated ZL adsorbent	11.9	39.2	32.75	99.56

The optimal conditions of MB removal by adsorption using raw and activated *Ziziphus lotus* material are respectively: an initial pH of 10.4/11.9, an adsorbent dosage of 760.9/390.2 mg/L, and a contact time of 38.60/32.75 min. The result of the RSM methodology based on validation data showed a R^2 of 0.99 for both the raw material and the activated carbon.

References

[1] Moroccan Public Water Domain, Research and water planning department, guide for developing effluents' specific limit values, 2009.

- [2] K. Singh, S. Arora, Removal of synthetic textile dyes from wastewaters: a critical review on present treatment technologies, *Crit. Rev. Env. Sci. Technol.*, 41 (2011) 807–878.
- [3] A.H. Jawad, S. Sabar, M.A.M. Ishak, L.D. Wilson, S.S.A. Norrahma, M.K. Talari, A.M. Farhan, Microwave assisted preparation of mesoporous activated carbon from coconut (Cocos nucifera) leaf by H_3PO_4 -activation for Methylene Blue adsorption, *Chem. Eng. Commun.*, 204 (2017) 1143–1156.
- [4] A.H. Jawad, R.A. Rashid, K. Ismail, S. Sabar, High surface area mesoporous activated carbon developed from coconut leaf by chemical activation with H_3PO_4 for adsorption of Methylene Blue, *Desal. Water Treat.*, 74 (2017) 326–335.
- [5] I.D. Mall, V.C. Srivastava, N.K. Agarwal, I.M. Mishra, Removal of congo red from aqueous solution by bagasse fly ash and activated carbon: kinetic study and equilibrium isotherm analyses, *Chemosphere*, 61 (2005) 492–501.
- [6] M.A. Ahmad, N. Ahmad, O.S. Bello, Adsorptive removal of malachite green dye using durian seed-based activated carbon, *Water. Air. Soil. Pollut.*, 225 (2014) 1–18.
- [7] R.C. Bansal, J.B. Donnet, F. Stoeckli, *Active carbon*. New York: Dekker, 1988.
- [8] H. Marsh, R. Menendez, *Introduction to carbon science*. London: Butterworths, 1989, pp. 37–73.
- [9] A.A. Ahmad, B.H. Hameed, N. Aziz, Adsorption of direct dye on palm ash: kinetic and equilibrium modeling, *J. Hazard. Mater.*, 141 (2007) 70–76.
- [10] C.S. Yang, Y.S. Jang, H.K. Jeong, Bamboo-based activated carbon for supercapacitor applications, *Curr. Appl. Phys.*, 14 (2014) 1616–1620.
- [11] B.H. Beakou, K.E. Hassani, M.A. Houssaini, M. Belbahloul, E. Oukani, A. Anouar, A novel biochar from *Manihot esculenta* Crantz waste: application for the removal of malachite green from wastewater and optimization of the adsorption process, *J. Wat. Sci. Tech.*, 76 (2017) 1447–1455.
- [12] A.H. Jawad, Carbonization of rubber (Heveabrasiliensis) seed shell by one-step liquid phase activation with H_2SO_4 for methylene blue adsorption, *Desal. Water Treat.*, 129 (2018) 279–288.
- [13] A.M. Arbabi, S. Hemati, Preparation of controlled porosity activated carbon from walnut shell for phenol adsorption Abbas, *Desal. Water Treat.*, 130 (2018) 63–70.
- [14] A. Shebl, A.M. Omer, T.M. Tamer, Adsorption of cationic dye using novel O-amine functionalized chitosan Schiff base derivatives: isotherm and kinetic studies, *Desal. Water Treat.*, 130 (2018) 132–141.
- [15] G.C. Ghosh, S. Zaman, T.K. Chakraborty, Adsorptive removal of Cr(VI) from aqueous solution using rice husk and rice husk ash Gopal Chandra, *Desal. Water Treat.*, 130 (2018) 151–160.
- [16] W. Boontham, S. Babel, Removal of lead from aqueous solution using low-cost adsorbents from Apiaceae family, *Desal. Water Treat.*, 130 (2018) 182–193.
- [17] S. Sahnoun, M. Boutahala, G. Fingueneisel, T. Zimny, A. Kahoul, Adsorption studies of an azo dye using polyaniline coated calcined layered double hydroxides, *Desal. Water Treat.*, 129 (2018) 255–265.
- [18] F. Zaha, R. Marouf, F. Ouadjenia, J. Schott, Kinetic and thermodynamic studies of the adsorption of Pb(II), Cr(III) and Cu(II) onto modified bentonite, *Desal. Water Treat.*, 131 (2018) 282–290.
- [19] A. Allaoui, Z. Hattab, R. Zerdoum, R. Djellabi, Y. Berredjem, W. Bessashi, K. Guerfi, Adsorption of hexavalent chromium by crushed brick: effect of operating parameters and modeling study, *Desal. Water Treat.*, 131 (2018) 291–304.
- [20] T. Islam, T. Ye, C. Peng, Adsorption of Eriochrome Black T dye using alginate crosslinked Prunus avium leaf mediated nanoparticles: characterization, optimization and equilibrium studies, *Desal. Water Treat.*, 131 (2018) 305–316.
- [21] Y. Zeng, W. Li, L. Wang, T. Du, J. Huang, Z. Huang, J. Wang, J. Tang, M. Wang, J. Wang, C. Jiang, P. Yang, Study on the kinetics of the adsorption of reactive brilliant red K-2BP onto modified soybean straw activated carbon, *Desal. Water Treat.*, 125 (2018) 302–309.
- [22] E. Jahandiez, R. Maire, *Catalogue des plantes du Maroc*. Imprimerie Minerva, Alger; Lechevalier, Paris. Vol. 2, 1932.
- [23] R. Negre, *Petite flore des régions arides du Maroc Occidental*. CNRS Edit., Paris. Vol. 2, 1962.
- [24] N. El Messaoudi, A. Dbik, M. El Khomri, A. Sabour, S. Bentahar, A. Lacherai, Date stones of *Phoenix dactylifera* and jujube shells of *Ziziphus lotus* as potential biosorbents for anionic dye removal, *Int. J. Phytorem.*, 19 (2017) 1047–1052.
- [25] S.L. Liu, Y.N. Wang, K.T. Lu, Preparation and pore characterization of activated carbon from Ma bamboo (*Dendrocalamus latiflorus*) by H_3PO_4 chemical activation, *J. Porous. Mat.*, 21 (2014) 459–66.
- [26] T. Ramesh, N. Rajalakshmi, K.S. Dhathathreyan, Activated carbons derived from tamarind seeds for hydrogen storage, *J. Energy Storage*, 4 (2015) 89–95.
- [27] V.K. Gupta, D. Pathania, S. Sharma, P. Singh, Preparation of bio-based porous carbon by microwave assisted phosphoric acid activation and its use for adsorption of Cr(VI), *J. Colloid. Interface. Sci.*, 401(2013) 125–132.
- [28] J. Xu, L. Chena, H. Qua, Y. Jiaoa, J. Xie, Preparation and characterization of activated carbon from reedy grassleaves by chemical activation with H_3PO_4 , *Appl. Sur. Sci.*, 320 (2014) 674–680.
- [29] E.N. El Qada, S.J. Allen, G.M. Walker, Influence of preparation conditions on the characteristics of activated carbons produced in laboratory and pilot scale systems, *Chem. Eng. J.*, 142 (2008) 1–13.
- [30] W.C. Lim, C. Srinivasakannan, N. Balasubramanian, Activation of palm shells by phosphoric acid impregnation for high yielding activated carbon, *J. Anal. Appl. Pyrol.*, 88 (2010) 181–186.
- [31] Y. Sun, H. Li, G. Li, B. Gao, Q. Yue, X. Li, Characterization and ciprofloxacin adsorption properties of activated carbons prepared from biomass wastes by H_3PO_4 activation, *Bioresour. Technol.*, 217 (2016) 239–244.
- [32] A. Hassani, L. Alidokht, A.R. Khataee, S. Karaca, Optimization of comparative removal of two structurally different basic dyes using coal as a low-cost and available adsorbent, *J. Taiwan. Inst. Chem. Eng.*, 45 (2014) 1597–1607.
- [33] A.H. Jawad, A.F.M. Alkarkhi, N.S.A. Mubarak, Photocatalytic decolorization of methylene blue by an immobilized TiO_2 film under visible light irradiation: Optimization using response surface methodology (RSM), *Desal. Water Treat.*, (2014) 1–12.
- [34] S. Chattoraj, N.K. Mondal, B. Das, P. Roy, B. Sadhukhan, Carbaryl removal from aqueous solution by Lemna major biomass using response surface methodology and artificial neural network, *J. Environ. Chem. Eng.*, 2 (2014) 1920–1928.
- [35] Z. Alam, S.A. Muyibi, J. Toramae, Statistical optimization of adsorption processes for removal of 2,4-dichlorophenol by activated carbon derived from oil palm empty fruit bunches, *J. Environ. Sci.*, 19 (2007) 674–677.
- [36] I.A.W. Tan, A.L. Ahmad, B.H. Hameed, Optimization of preparation conditions for activated carbons from coconut husk using response surface methodology, *Chem. Eng. J.*, 137 (2008) 462–470.
- [37] R.H. Myers, D.C. Montgomery, *Response Surface Methodology: Product and Process Optimization Using Designed Experiments*. 2nded., John Wiley & Sons, New York, 2002.
- [38] P. Ricou-Hoeffler, I. Lecuyer, P.L. Cloirec, Experimental design methodology applied to adsorption of metallic ions onto fly ash, *Water Res.*, 35 (2001) 965–976.
- [39] D.C. Montgomery, *Design and Analysis of Experiments*, 5th ed., John Wiley & Sons, New York, 2001.
- [40] K. Yetilmmezsoy, S. Demirel, R.J. Vanderbei, Response surface modeling of Pb(II) removal from aqueous solution by Pistacia-vera L.: Box–Behnken experimental design, *J. Hazard. Mater.*, 171 (2009) 551–562.
- [41] S. Yorgun, N. Vural, H. Demiral, Preparation of high-surface area activated carbons from Paulownia wood by $ZnCl_2$ activation, *Micropor. Mesopor. Mater.*, 122 (2009) 189–194.
- [42] J.H. Tay, X.G. Chen, S. Jeyaseelan, N. Graham, Optimising the preparation of activated carbon from digested sewage sludge and coconut husk, *Chemosphere*, 44 (2001) 45–51.

- [43] D. Wu, J. Zhou, Y. Li, Effect of the sulfidation process on the mechanical properties of a CoMoP/Al₂O₃ hydrotreating catalyst, *Chem. Eng. Sci.*, 64 (2009) 198–206.
- [44] A.C. Lua, T. Yang, Effect of activation temperature on the textural and chemical properties of potassium hydroxide activated carbon prepared from pistachio-nut shell, *J. Colloid. Interface. Sci.*, 274 (2004) 594–601.
- [45] M. Myglovets, O.I. Poddubnaya, O. Sevastyanova, M.E. Lindström, B. Gawdzik, M. Sobiesiak, M.M. Tsyba, V.I. Sapsay, D.O. Klymchuk, A.M. Puziy, Preparation of carbon adsorbents from lignosulfonate by phosphoric acid activation for the adsorption of metal ions, *J. Carbon.*, 80 (2014) 771–783.
- [46] C.H. Weng, Y.T. Lin, T.W. Tzeng, Removal of Methylene Blue from aqueous solution by adsorption onto pineapple leaf powder, *J. Hazard. Mater.*, 170 (2009) 417–424.
- [47] Y. Chen, B. Huang, M. Huang, B. Cai, The preparation and characterization of activated carbon from mango steen shell, *J. Taiwan. Inst. Chem. Eng.*, 42 (2011) 837–842.
- [48] S.F. Dyke, A.J. Floyd, M. Sainsbury, R.S. Theobald, *Organic Spectroscopy: An Introduction*, 1st ed., Penguin Books, Ringwood, Victoria, Australia, 1971.
- [49] K.Y. Foo, B.H. Hameed, Utilization of biodiesel waste as a renewable resource for activated carbon: Application to environmental problems, *J. Renew. Sust. Energ. Rev.*, 13 (2009) 2495–2504.
- [50] Z. Ryu, H. Rong, J. Zheng, M. Wang, B. Zhang, Microstructure and chemical analysis of PAN-based activated carbon fibers prepared by different activation methods, *J. Carbon.*, 40 (2002) 1144–1147.
- [51] J.L. Figueiredo, M.F.R. Pereira, M.M.A. Freitas, J.J.M. Orfao, Modification of the surface chemistry of activated carbons, *J. Carbon.*, 37 (1999) 1379–1389.
- [52] J. Zheng, Q. Zhao, Z. Ye, Preparation and characterization of activated carbon fiber (ACF) from cotton woven waste, *J. Appl. Surf. Sci.*, 299 (2014) 86–91.
- [53] A.L. Cazetta, A.M.M. Vargas, E.M. Nogami, M.H. Kunita, M.R. Guilherme, A.C. Martins, T.L. Silva, J.C.G. Moraes, V.C. Almeida, NaOH-activated carbon of high surface area produced from coconut shell: Kinetics and equilibrium studies from the Methylene Blue adsorption, *J. Chem. Eng.*, 174 (2011) 117–125.
- [54] R. Baccar, J. Bouzid, M. Feki, A. Montiel, Preparation of activated carbon from Tunisian olive-waste cakes and its application for adsorption of heavy metal ions, *J. Hazard. Mater.*, 162 (2009) 1522–1529.
- [55] E.W. Shin, R.M. Rowell, Cadmium ion sorption onto lignocellulosic biosorbent modified by sulfonation: the origin of sorption capacity improvement, *J. Chemosphere*, 60 (2005) 1054–1061.
- [56] Y. Chen, C. Xiong, Adsorptive removal of As (III) ions from water using spent grain modified by polyacrylamide, *J. Environ. Sci.*, 45 (2016) 124–130.
- [57] A. Omri, M. Benzina, Characterization of activated carbon prepared from a new raw lignocellulosic material: ziziphus spina-christi seeds, *J. Soc. Chim. Tunis.*, 14 (2012) 175–183.
- [58] H.P. Khalil, M. Jawaid, P. Firoozian, U. Rashid, Activated carbon from various agricultural wastes by chemical activation with KOH: preparation and characterization activated carbon from various agricultural wastes, *J. Biobased. Mater. Bioenergy*, 7 (2013) 708–714.
- [59] X. Wang, X. Liang, Y. Wang, Xi, Wang, M. Liu, D. Yin, S. Xia, J. Zhao, Y. Zhang, Adsorption of Copper (II) onto activated carbons from sewage sludge by microwave-induced phosphoric acid and zinc chloride activation, *Desalination*, 278 (2011) 231–237.
- [60] C.M. Gonza, S. Roma, E. Sabio, F. Zamora, J.F. Gonza, Characterisation under static and dynamic conditions of commercial activated carbons for their use in wastewater plants, *J. Appl. Surf. Sci.*, 252 (2006) 6058–6063.
- [61] S.M. Anisuzzaman, C.G. Joseph, W.M. Ashri, D. Krishnaiah, S.Y. Ho, Preparation and characterization of activated carbon from *Typhaorientalis* leaves, *Int. J. Ind. Chem.*, 6 (2015) 9–21.
- [62] Bonomo, L, *Wastewater Treatment*, Mc Graw Hill Education, Italy, 2008.
- [63] A.M.M. Vargas, A.L. Cazetta, C.A. Garcia, J.C.G. Moraes, E.M. Nogami, E. Lenzi, W.F. Costa, V.C. Almeida, Preparation and characterization of activated carbon from a new raw lignocellulosic material: flamboyant (*Delonixregia*) pods, *J. Environ. Manage.*, 92 (2011) 178–184.
- [64] H. Higuti, P.A. Silva, J. Papp, V.M.O. Okiyama, E.A. Andrade, A.A. Marcondes, A.J. Nascimento, Colourimetric determination of cyclodextrins and studies on optimisation of CGTase production from *B. firmus* using factorial designs, *Braz. Arch. Biol. Technol.*, 47 (2004) 837–841.
- [65] R. Azargohar, A.K. Dalai, Production of activated carbon from Luscar char: experimental and modelling studies, *Micropor. Mesopor. Mater.*, 85 (2005) 219–225.
- [66] B.H. Hameed, Evaluation of papaya seed as a novel non-conventional low-cost adsorbent for removal of methylene blue, *J. Hazard. Mater.*, 162 (2010) 939–994.